

Quantum fluctuations of a nearly critical Heisenberg spin glass

A. Georges,¹ O. Parcollet,² and S. Sachdev³

¹*Laboratoire de Physique Théorique, Ecole Normale Supérieure, 24 Rue Lhomond 75005, Paris, France*

²*Center for Material Theory, Department of Physics and Astronomy, Rutgers University, Piscataway, New Jersey 08854*

³*Department of Physics, Yale University, New Haven, Connecticut 06520*

(Received 25 September 2000; published 1 March 2001)

We describe the interplay of quantum and thermal fluctuations in the infinite-range Heisenberg spin glass. This model is generalized to $SU(N)$ symmetry, and we describe the phase diagram as a function of the spin S and temperature T . The model is solved in the large- N limit, and certain universal critical properties are shown to hold to all orders in $1/N$. For large S , the ground state is a spin glass, but quantum effects are crucial in determining the low- T thermodynamics: we find a specific heat linear in T and a local spectral density of spin excitations, $\chi''_{loc}(\omega) \sim \omega$ for a spin-glass state which is marginally stable to fluctuations in the replicon modes. For small S , the spin-glass order is fragile, and a spin-liquid state with $\chi''_{loc} \sim \tanh(\omega/2T)$ dominates the properties over a significant range of T and ω . We argue that the latter state may be relevant in understanding the properties of strongly disordered transition-metal and rare-earth compounds.

DOI: 10.1103/PhysRevB.63.134406

PACS number(s): 75.10.Nr, 64.60.Cn

I. INTRODUCTION

The study of intermetallic compounds of the transition metals and rare earths has been a subject at the forefront of condensed matter physics for some time now.^{1,2} A rich and complex variety of behaviors is observed in low-temperature electrical and magnetic measurements, much of which lacks a comprehensive theoretical description. The complexity arises from the dominant role played by the local magnetic moments on the d and f orbitals and their interactions with each other and the itinerant charge carriers.

It is convenient to begin our discussion in a phase with well-established magnetic order, in which each magnetic moment is effectively static. This static moment could be polarized in a regular manner (as in a commensurate antiferromagnet or an incommensurate spin-density wave) or point in random directions (as in a spin-glass state). In most realistic systems, the magnetic moment is either quite small or has averaged to zero by dynamic quantum fluctuations: so it is useful to consider mechanisms which reduce the magnetic moment and eventually cause it to vanish at a quantum phase transition to some paramagnetic state. Two distinct routes to such a quantum phase transition can be envisaged, and, we believe, the interplay between them is at the heart of the complexity of the problem. In the first route, originally discussed by Doniach,³ the moment is quenched by Kondo screening by the itinerant electrons: theories of such quantum critical points have been proposed⁴⁻⁷ in which the predominant role of the itinerancy is to overdamp the collective magnetic excitations. In the second route, the exchange interactions between the moments play a more fundamental role: a pair of spins interacting with an antiferromagnetic exchange prefers to form a singlet valence bond, and the proliferation of such singlets can destroy the magnetic order. Analytic theories for such transitions has been made mainly for systems without quenched disorder.⁸ Simple models of crossovers between these two routes have also been presented.⁹⁻¹¹

This paper will present a detailed study of the second

route to destruction of magnetic order for the case of a strongly random system with spin-glass magnetic order. There are a number of motivations for focusing on random systems. First, randomness is inevitably present in all materials, and it is clear that it strongly perturbs the low-temperature properties. Spin-glass order is present in a number of systems, while others appear to be in the vicinity of such a state. Finally, a technical motivation is in the structure of the mean-field theory we shall present: it builds an important feedback effect between the intersite magnetic correlations and the single-site spin dynamics, and this is crucial to all the nontrivial spin correlations we shall describe. Such a feedback is absent in previous studies of the magnetic quantum critical point, and it has been argued that this is an important limitation for them.^{7,11} A different route to incorporating these feedback effects has been taken in some recent studies;¹² however, they discuss only the paramagnetic state of their model, and the extent to which magnetically ordered states preempt their results remains to be clarified.

This paper is organized as follows: In Sec. II we present our spin-glass model and give an outline of our results, including the phase diagram. Section III is devoted to the nature of the paramagnetic solutions and, more specifically, to the quantum critical regime. Section IV is devoted to the spin-glass phase and to the various regimes within this phase, as a function of temperature and of the size of the spin. The Appendixes contain technical details and some additional results on the quantum rotor and Ising spin glasses of Ref. 13.

II. MODEL AND OUTLINE OF THE RESULTS

The numerous recent studies of quantum fluctuations in spin glasses¹⁴ have focused either on infinite-range models of Ising and rotor models^{13,15} or models in low dimensions which flow to strong disorder fixed points.¹⁶⁻¹⁸ Here we shall continue the study of infinite-range models, but will consider a model of Heisenberg spins: in this case, the path integral for each spin has a important Berry phase term which im-

poses the spin commutation relations. As we will see, this leads to a great deal of new physics¹⁹ and nontrivial dynamic spin correlations even in the spin-glass state. More specifically, we present a complete solution of the quantum Heisenberg spin glass on a fully connected lattice of \mathcal{N} sites with strong Gaussian disorder, both in the paramagnetic and glassy phases, when the spin-symmetry group is extended from $SU(2)$ to $SU(N)$ and the large- N limit is taken. In the limit of large connectivity, (dynamical) mean-field techniques apply and the model can be reduced to the study of a self-consistent single-site problem, which is, however, still highly nontrivial because of quantum effects. The large- N limit is instrumental in allowing for an explicit solution. Nevertheless, some of our results regarding the quantum-critical regime have been extended beyond the large- N limit. In a recent publication,²⁰ we summarized the main results of the present study. Here we provide detailed derivations and new results, such as a full discussion of the paramagnetic phases and a discussion beyond large N .

The model considered in this paper is defined by the Hamiltonian

$$H = \frac{1}{\sqrt{\mathcal{N}\mathcal{N}}} \sum_{i < j} J_{ij} \vec{S}_i \cdot \vec{S}_j, \quad (1)$$

where the magnetic exchange couplings J_{ij} are independent, quenched random variables distributed according to a Gaussian distribution

$$P(J_{ij}) = \frac{1}{J\sqrt{2\pi}} e^{-J_{ij}^2/(2J^2)}. \quad (2)$$

As already pointed out by Bray and Moore,²¹ after using the replica trick to average over the disorder,²² the mean-field (infinite-dimensional) limit maps the model onto a *self-consistent single site model* with the action (in imaginary time τ , with β the inverse temperature)

$$S_{\text{eff}} = S_B - \frac{J^2}{2N} \int_0^\beta d\tau d\tau' Q^{ab}(\tau - \tau') \vec{S}^a(\tau) \cdot \vec{S}^b(\tau') \quad (3)$$

and the self-consistency condition

$$Q^{ab}(\tau - \tau') = \frac{1}{N^2} \langle \vec{S}^a(\tau) \cdot \vec{S}^b(\tau') \rangle_{S_{\text{eff}}}, \quad (4)$$

where $a, b = 1, \dots, n$ denote the replica indices (the limit $n \rightarrow 0$ has to be taken later) and S_B is the Berry phase of the spin.¹⁹ Due to their time dependence, the solution of these mean-field equations remains a very difficult problem for $N = 2$, even in the paramagnetic phase. Thus, in Ref. 21, as well as in most subsequent work,²³ the *static approximation* was used, neglecting the τ dependence of $Q^{ab}(\tau)$. This approximation may be reasonable in some regimes, but prevents a study of the quantum equilibrium dynamics and is particularly inappropriate in the quantum-critical regime. However, this imaginary time dynamics has been explicitly studied in a quantum Monte Carlo simulation *in the paramagnetic phase* with spin $S = 1/2$ by Grempel and Rozenberg.²⁴ Recently, we introduced a large- N solution of

the mean-field problem,²⁰ in which the problem is exactly solvable and, as explained below, the solution provides a good description of the physics of the $N = 2$ mean-field model, to the extent the latter is understood. More specifically, in the following we will consider two different types of spin representations for the $SU(N)$ spins.

(a) *Bosonic* representations. The spin operator S is represented using Schwinger bosons b by $S_{\alpha\beta} = b_\alpha^\dagger b_\beta - S \delta_{\alpha\beta}$, with the constraint $\sum_\alpha b_\alpha^\dagger b_\alpha = SN$ ($0 \leq S$). In the language of Young tableaux, these representations are described by one line of length SN . They are a natural generalization of an $SU(2)$ spin of size S .

(b) *Fermionic* representations. The spin operator S is represented using Abrikosov fermions f by $S_{\alpha\beta} = f_\alpha^\dagger f_\beta - q_0 \delta_{\alpha\beta}$, with the constraint $\sum_\alpha f_\alpha^\dagger f_\alpha = q_0 N$ ($0 \leq q_0 \leq 1$). In the language of Young tableaux, these representations are described by one column of length $q_0 N$. Note that for $SU(2)$, only $S = 0$ and $S = 1/2$ can be represented in this manner.

In the following, we refer to the model with bosonic (fermionic) representations as the bosonic (fermionic) model. In the fermionic model, quantum fluctuations are so strong in large N that the spin-glass ordering is destroyed,¹⁹ contrary to the bosonic model, where a spin-glass phase exists, as explained below. The two models have different theoretical interest: if one wants to concentrate on the quantum-critical regime, above the spin-glass ordering temperature, one can use the fermionic model (as, e.g., in Ref. 25). However, since we are interested in the spin-glass phase itself, we will now focus on the bosonic model. Nevertheless, our results on the paramagnet will be valid for both cases with only slight modifications explicitly quoted below.

In the $N \rightarrow \infty$ limit, the mean field self-consistent model (3) reduces to an integral equation for the Green's function of the boson $G_b^{ab}(\tau) = -\langle T b^a(\tau) b^{\dagger b}(0) \rangle$ where the overbar denotes the average over disorder and the brackets the thermal average:¹⁹

$$(G_b^{-1})^{ab}(i\nu_n) = i\nu_n \delta_{ab} + \lambda^a \delta_{ab} - \Sigma_b^{ab}(i\nu_n), \quad (5a)$$

$$\Sigma_b^{ab}(\tau) = J^2 [G_b^{ab}(\tau)]^2 G_b^{ab}(-\tau), \quad (5b)$$

$$G_b^{aa}(\tau = 0^-) = -S. \quad (5c)$$

Similarly for the fermionic model, we have

$$(G_f^{-1})^{ab}(i\omega_n) = i\omega_n \delta_{ab} + \lambda^a \delta_{ab} - \Sigma_f^{ab}(i\omega_n), \quad (6a)$$

$$\Sigma_f^{ab}(\tau) = -J^2 (G_f^{ab}(\tau))^2 G_f^{ab}(-\tau), \quad (6b)$$

$$G_f^{aa}(\tau = 0^-) = q_0. \quad (6c)$$

In these equations, $\nu(\omega)$ are the bosonic (fermionic) Matsubara frequencies and the inversion should be taken with respect to the replica indices a, b . Note that our conventions for the sign of the Green's functions in this paper slightly differ from those of Ref. 19. Note that, although the equations are written in term of G , the physical quantity is the *local* spin susceptibility $\chi_{\text{loc}}(\tau) = \langle S(\tau) S(0) \rangle$, which is given in the large- N limit by

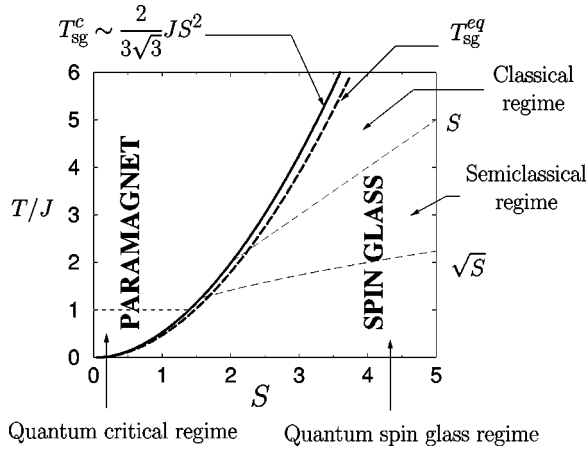


FIG. 1. Phase diagram of the mean-field bosonic model. There is a spin-glass phase below the spin-glass temperature T_{sg}^c , which is determined with the marginality condition (see Sec. IV). $T_{\text{sg}}^{\text{eq}}$ is the spin-glass temperature as determined by the stationarity criterion.

$$\chi_{\text{loc}}(\tau) = G_b^{aa}(\tau)G_b^{aa}(-\tau). \quad (7)$$

In many instances below (where we mostly focus on the bosonic case), we shall drop the index b in G_b .

From both analytical and numerical analyses of these integral equations, we have constructed the phase diagram displayed in Fig. 1, as a function of the size of the spin S and temperature T . Let us give here a brief overview of the main features of this phase diagram, which will be studied in great detail in the rest of this paper. As is evident from Fig. 1, it is useful to divide the discussion into models with S large and S small. Both regimes are accessible in the large- N limit, where S is effectively a continuous parameter taking all positive values. For the physical case $N=2$, we will present evidence later that at least $S=1/2$ is in the small- S regime for the infinite-range model; moreover, we can expect that at least some of the consequences of increased quantum fluctuations in a realistic model with finite-range interactions are mimicked by taking small- S values in the large- N theory of the infinite-range model.

For large S , the ground state must clearly be a spin glass (Fig. 1). However, even for very large S , it is necessary to consider quantum effects in understanding the low- T excitations and thermodynamics, and these have not been previously described. In this paper (Secs. IVC 2 and IVD), we will show that the local spin susceptibility has a low-energy density of states which increases linearly with energy. At the same time, the specific heat also has a linear dependence upon temperature. These results hold for temperatures $T < J\sqrt{S}$, although characteristic excitations have an energy of order JS for $T < JS$; we will provide scaling functions which determine the dynamic response functions at these energies. At even higher T , there is a phase transition to a paramagnet at $T \sim JS^2$. For large S the static properties of this phase transition are well described by a purely classical theory in which the \vec{S} in Eq. (1) are commuting vectors of length S . Notice also that we indicate two critical temperatures T_{sg}^c and $T_{\text{sg}}^{\text{eq}}$: as we discuss in Sec. IV, these are a consequence of

peculiarities in the nature of replica symmetry breaking, where the dynamic freezing into the spin-glass phase (T_{sg}^c) happens at a slightly higher temperature than the equilibrium transition ($T_{\text{sg}}^{\text{eq}}$).

For small S , we also find a spin-glass phase (Fig. 1) at $T=0$, but the order vanishes at a small T . Moreover, its excitations and finite- T properties are very different from those at large S . These are now dominated by signals of a ‘‘spin-liquid’’ state discussed in Ref. 19 and described in Sec. III A. In particular, we describe a quantum-critical region in the paramagnet where $\max(\omega, T)$ is the characteristic energy scale and the local dynamic spin susceptibility obeys $\chi_{\text{loc}}''(\omega) \sim \tanh(\omega/2T)$. We believe that aspects of this regime may be relevant to disordered transition-metal and rare-earth compounds where exchange interactions between the magnetic moments are playing a dominant role. Completion of this picture requires an understanding of the stability of the ‘‘spin-liquid’’ picture to mobile charge carriers and this has also been addressed in a previous work.²⁵

III. PARAMAGNETIC PHASE

Contrary to the classical case, the paramagnetic phase of quantum spin-glass models is nontrivial in mean-field theory. An early discussion of these solutions has been given in Ref. 19, but we present here a much more complete description and compare our results to the $N=2$ case, when numerical results are available. Since in this section we look for paramagnetic solutions, we will consider only *replica-diagonal* solutions of Eqs. (5): $G^{ab} \propto \delta_{ab}$. Two types of paramagnetic solutions have been found, which we will now consider successively: the *spin-liquid* solutions and the *local moment* solutions.

A. Spin-liquid solutions

1. Large- N limit

A low-frequency, long-time analysis of the integral equations (5) reveals that, under the condition that $\lambda - \Sigma(i0^+)$ vanish at low temperature, a solution can be found which displays a power-law decay of the Green’s function at long time:¹⁹ $G(\tau) \sim 1/\sqrt{\tau}$. These solutions display a singularity in the complex plane of frequencies, z , at $z=0$, with an amplitude which can be parametrized by an angle θ as

$$G(z) \sim \frac{Ae^{-i\pi/4-i\theta}}{\sqrt{z}} \quad \text{for } z \rightarrow 0, \quad \text{Im } z \rightarrow 0. \quad (8)$$

(Values of z on the imaginary frequency axis at the Matsubara frequencies will be denoted by ν_n , while on the real axis will be denoted ω .) Thus these solutions display a slow local spin dynamics: $\text{Im } \chi_{\text{loc}}(\omega) \propto \text{sgn } \omega$ for $\omega \rightarrow 0$, $T=0$. Moreover, the *local* susceptibility $\chi_{\text{loc}}(T) \equiv \int_0^\beta \chi_{\text{loc}}(\tau) d\tau$ diverges as $\chi_{\text{loc}}(T) \sim \ln T/J$ at low temperature. More precisely, one can find the thermal scaling function characterizing the $\tau \rightarrow \infty$, $T \rightarrow 0$ limit, as explained in a previous paper²⁵:

$$\chi_{\text{loc}}(\tau, \beta) \propto \left(\frac{\pi/\beta}{\sin \pi\tau/\beta} \right) + \dots, \quad J\chi_{\text{loc}}''(\omega, T) \propto \tanh \frac{\omega}{2T}. \quad (9)$$

Note that in the paramagnetic phase of *quantum* models, the local susceptibility $\chi_{\text{loc}}(T)$ (which is the response to a *local* magnetic field) differs from the uniform susceptibility $\chi(T)$ (response to a constant magnetic field), contrary to *classical* spin-glass models where $\chi = \chi_{\text{loc}}$ (Ref. 22): This is a consequence of the commutation relations of the spin, as can be seen, for example, in the high-temperature expansion in the SU(2) model. In this large- N limit, it can be shown that $\chi(T) \ll \chi_{\text{loc}}(T)$ for $T \rightarrow 0$ and numerical computations indeed suggest that $\chi(T) \sim \text{const.}$ ²⁵

Remarkably, the parameter θ which characterizes the *spectral asymmetry*²⁶ of the spectral density at low frequency can be explicitly related to the size S of the spin (which involves *a priori* an integral of the spectral density over all frequencies). This is very similar to a kind of Friedel sum rule applying to this problem, and indeed the derivation follows a very similar route, based on the existence of a Luttinger-Ward functional. (Interestingly enough, the ‘‘boundary term’’ which usually vanishes in such derivations contributes here a finite value.) This derivation is presented in detail in Appendix A, where the following relation between θ and S is established:

$$\frac{\theta}{\pi} + \frac{\sin 2\theta}{4} = \begin{cases} \frac{1}{2} + S & \text{in the bosonic model} \\ \frac{1}{2} - q_0 & \text{in the fermionic model.} \end{cases} \quad (10)$$

This relation has important consequences for the physical properties of the spin-liquid solutions. First, we note that the spectral density must obey the positivity conditions $\text{Im} G_f(\omega + i0^+) < 0$ and $\text{sgn}(\omega)\text{Im} G_b(\omega + i0^+) < 0$. Hence, in the fermionic case, θ must obey $-\pi/4 \leq \theta \leq \pi/4$. It is easily checked from Eq. (10) that θ precisely describes this range of parameters as q_0 is varied from $q_0 = 0$ to $q_0 = 1$ and that the $\theta(q_0)$ relation is unique. This suggests that the spin-liquid solution is an acceptable low-temperature solutions for the whole range of q_0 in the fermionic case. In contrast, in the bosonic case, the plot in Fig. 2 shows that (10) actually defines *two* values of θ (in the allowed range $\pi/4 \leq \theta \leq 3\pi/4$) for a given spin S as long as $S < S_{\text{max}} \approx 0.052$, while no value of θ is found for $S > S_{\text{max}}$. This implies that no paramagnetic solution of the spin-liquid type is found *at zero temperature* in the bosonic case as soon as $S > S_{\text{max}}$ (note that furthermore S_{max} is very small). For $S < S_{\text{max}}$, such solutions exist at zero temperature (even though they are not the true ground state: see below) with the locally stable solution corresponding to the smallest of the two values of θ . However, even for $S > S_{\text{max}}$, *at low ($T < J$) but finite temperature*, the spin-liquid solutions do exist in the bosonic model. By this, we mean that a numerical computation in imaginary time gives a solution which exhibits the scaling form (9), for which a unambiguous value of the spectral asymmetry θ can be defined and computed numerically. At very low temperature, these

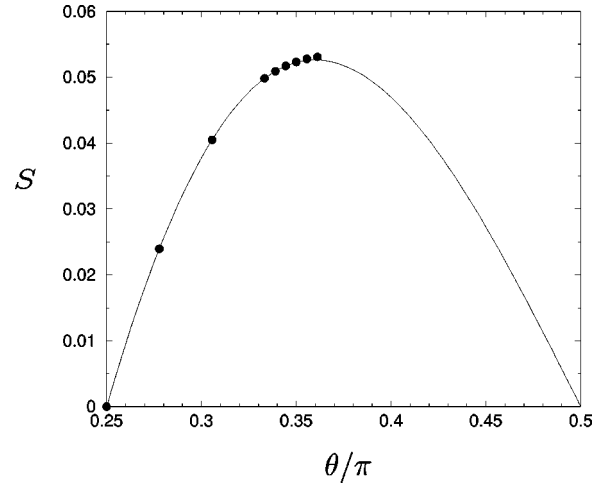


FIG. 2. S as a function of θ for the bosonic model. The solid line is given by relation (10) and the points were obtained previously from a numerical solution of the saddle-point equation at zero temperature (Ref. 19).

solutions are unstable to the spin-glass solution, but above the spin-glass temperature at low spin, they are relevant in the quantum-critical regime associated with the quantum-critical point at $S = 0$. We shall comment in more detail, at the end of the following section, on the nature of the paramagnetic solutions found at low temperature for small values of S , in the bosonic case.

Another consequence of relation (10) is that it allows one to predict that these spin-liquid solutions have a *nonzero extensive entropy* at zero temperature and to calculate the value of this entropy analytically. The derivation of this result follows very closely a similar analysis of the overscreened multichannel Kondo problem in the large- N limit, performed in Refs. 26 and 27, and only the main steps will be repeated here. This can be done either in the bosonic model or in the fermionic one, with slight modifications. Since the spin-liquid solutions are relevant at zero temperature only in the fermionic model, we shall present the result in this case. First, denoting by S the value of the entropy per spin at zero temperature, one establishes the following thermodynamic equality:

$$\frac{\partial S}{\partial q_0} = - \left. \frac{\partial \lambda}{\partial T} \right|_{T=0}. \quad (11)$$

Then a low-temperature expansion is used which allows one to relate the slope of $\lambda(T)$ to the spectral asymmetry parameter θ above, so that one finally gets (in the fermionic case)

$$\frac{\partial S}{\partial q_0} = \ln \frac{\sin(\pi/4 - \theta)}{\sin(\theta + \pi/4)}. \quad (12)$$

The entropy is then obtained by integration over the size of the spin, with the physically obvious boundary conditions $S(q_0 = 0) = S(q_0 = 1) = 0$. The resulting value of the entropy as a function of q_0 is plotted in Fig. 3.

Finally, we comment on the physical nature of the spin-liquid paramagnetic solutions found in this section. These

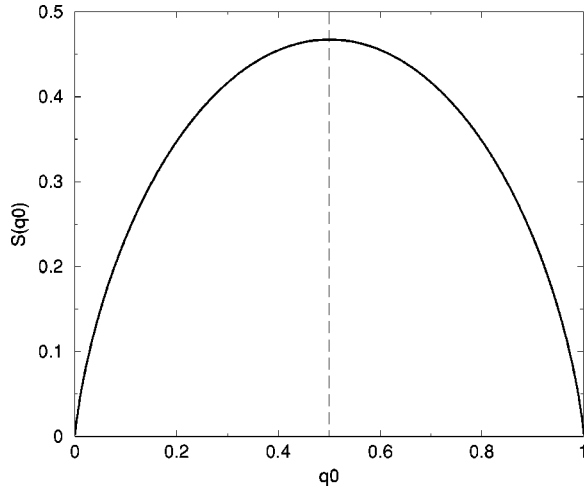


FIG. 3. Entropy as a function of the size of the spin (q_0) in the fermionic model.

solutions correspond to a partial screening of the local moment at each site, due to the interaction with the other spins. As a result, the local susceptibility diverges logarithmically (much slower than a Curie law), but an extensive entropy is still present at $T=0$, indicating a degenerate state. From a local point of view, the physics is somewhat similar to an overscreened Kondo system, but here the gapless bath which quenches the spin is not external, but self-consistently generated by the other spins. We suspect that the physics of this phase has to do with the degeneracy of the (large- N generalization) of the ‘‘triplet’’ state in which two spins are bound whenever a strong ferromagnetic bond J_{ij} is encountered. In Sec. III A 2, we show that this spin-liquid regime is not a peculiarity of the large- N limit, but indeed survives in the mean-field description of the quantum-critical regime of a $SU(2)$ quantum Heisenberg spin glass. It would be very valuable to gain a more direct understanding of this gapless spin-liquid regime from a study of the problem for a fixed configuration of bonds before averaging over disorder. This could be achieved numerically and is left for future studies.

2. Beyond the large- N limit

This subsection will show how recent renormalization group analyses of related models^{11,28,29} imply that the above spin-liquid solution applies to all orders in $1/N$. In particular, the large- N solution with $\text{Im } \chi_{\text{loc}} \propto \text{sgn } \omega$ for small ω acquires no corrections to its functional form: the only changes are to the nonuniversal proportionality constant. All the discussion below will be in a paramagnetic phase where it is sufficient to consider only a single replica, and so we will drop replica indices in this subsection.

We begin by rewriting Eq. (3) in the following form¹¹

$$S_{\text{eff}} = S_B - \gamma_0 \int_0^\beta d\tau \vec{S}(\tau) \cdot \vec{\phi}(\tau), \quad (13)$$

where γ_0 is a coupling constant and $\vec{\phi}$ is an annealed Gaussian random field with $\langle \vec{\phi}(\tau) \cdot \vec{\phi}(0) \rangle = 1/|\tau|^{2-\epsilon}$. It is reasonable to expect that the spin correlations in the quantum en-

semble defined by Eq. (13) decay with the power law $\langle \vec{S}(\tau) \cdot \vec{S}(0) \rangle \sim 1/|\tau|^\sigma$, and we are interested in determining the value of the exponent σ . A simple extension¹⁹ of the solution discussed above implies that in the large- N limit $\sigma = \epsilon$. Here we will argue that this equality is in fact *exact for all N* . Now using the self-consistency condition (4), we obtain $\sigma = \epsilon = 1$, which then implies $\text{Im } \chi_{\text{loc}} \propto \text{sgn } \omega$.

The field-theoretic renormalization group analysis of Eq. (13) was discussed in Ref. 29, and we will highlight the main results. The key observation is that renormalization of the theory (13) requires only a single wave-function renormalization factor Z and that there is no independent renormalization of the coupling constant γ_0 . This result was established diagrammatically in Ref. 29, and we will not reproduce the argument here. So if we renormalize the spin by $\vec{S} = \sqrt{Z} \vec{S}_R$, then the coupling constant renormalization is simply $\gamma_0 = \mu^{\epsilon/2} \gamma / \sqrt{Z}$, where μ is a renormalization scale. The renormalization constant is in general a complicated function of γ and was determined to two-loop order in Ref. 29:

$$Z = 1 - \frac{2\gamma^2}{\epsilon} + \frac{\gamma^4}{\epsilon} + \dots \quad (14)$$

in a minimal subtraction scheme. However, even though Z is not known exactly, the exponent σ can be determined exactly. Standard field-theoretical technology shows that the above renormalizations imply the β function

$$\beta(\gamma) = -\frac{\epsilon\gamma}{2} \left(1 - \frac{1}{2} \frac{\partial \ln Z}{\partial \ln \gamma} \right)^{-1}. \quad (15)$$

Furthermore, the exponent σ is given by the value of

$$\sigma(\gamma) = \beta(\gamma) \frac{\partial \ln Z}{\partial \gamma} \quad (16)$$

at the fixed point $\gamma = \gamma^*$ where $\beta(\gamma)$ vanishes. Comparing Eqs. (15) and (16), we see that

$$\beta(\gamma) = -[\epsilon - \sigma(\gamma)]\gamma/2. \quad (17)$$

Clearly, a zero of the β function must have $\sigma = \epsilon$, and this establishes the required result.

We note that similar examples of a critical exponent being valid to all orders (in spite of a nontrivial β function) can be found for other models in the statistical mechanics of disordered systems (see, e.g., Refs. 30 and 31).

B. ‘‘Local moment’’ solutions

In a mean-field model, one usually expects to find locally stable (while possibly unstable to ordering) paramagnetic solutions of the mean-field equations down to zero temperature. Hence the absence of solutions of the spin-liquid type for $S > S_{\text{max}}$ suggests that a different kind of paramagnetic solution should exist for those values of the spin. Indeed, we have found that the integral equations (5) have another class of paramagnetic solutions in the bosonic case. These solutions actually exist for all values of the spin S and down to zero temperature. Hence they coexist at low S with the spin-

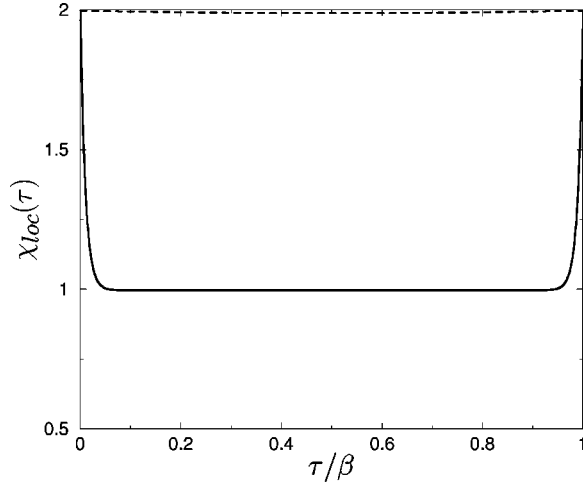


FIG. 4. $\chi_{\text{loc}}(\tau)$ extracted from a numerical solution of saddle point equations (5) in imaginary time, for $S=1$, $J=1$. The solid curve is low temperature ($J\beta=10$), and the dashed curve is high temperature ($J\beta=0.1$); for intermediate temperatures, the curves interpolate between the two.

liquid solutions in some range of temperature. Their physical nature is very different from the previous spin-liquid solutions, and as discussed below, they are not very physical solutions when considered at low temperature. They are characterized by a Green's function which does not decay at long times and obeys the asymptotic behavior $G_b(\tau) \approx -S - e^{-J^2\beta S^3\tau}$. In contrast to the spin-liquid case, λ diverges for $T \rightarrow 0$ in this regime:

$$\lambda \sim \frac{J^2 S^2}{T}. \quad (18)$$

Finding numerically these solutions of Eqs. (5) requires some care. We have used an algorithm in which we solve Eqs. (5) in imaginary time for $G(\tau)$, for a fixed value of $r = \int_0^\beta G(\tau) d\tau$, and then adjust the number of particles to S by a dichotomy on r . The local susceptibility $\chi_{\text{loc}}(\tau)$ obtained in this manner is displayed in Fig. 4. At high temperature, we find $\chi_{\text{loc}}(T) = S(S+1)/T$ as expected since the spin is essentially free. At low temperature, we find another Curie law, with a reduction of the Curie constant due to quantum fluctuations:

$$\chi_{\text{loc}}(T) = \frac{S^2}{T} \quad \text{for } T \rightarrow 0. \quad (19)$$

Hence, for these solutions, the effect of the interactions with the other spins is not strong enough to result in a qualitatively different screening regime, resulting merely in a reduction of the Curie constant. This is analogous to an *underscreened* Kondo regime.

These solutions are of a similar type as those found in in a quantum Monte Carlo simulation of the SU(2) mode.²⁴ There, also, a reduction of the Curie constant from $S(S+1)/3$ to $S^2/3$ was clearly observed. Thus, contrary to one of the conclusions of Ref. 24, the large- N limit correctly reproduces the paramagnetic local moment solution found for the

physical $N=2$ case. Moreover, a numerical solution of the large- N integral equations (5) for real frequencies can also be obtained both at high and low temperatures. The results are presented in Fig. 5 for both $\rho_b(\omega) \equiv -1/\pi \text{Im } G_b(\omega)$ and $\chi''_{\text{loc}}(\omega) \equiv 1/\pi \text{Im } \chi_{\text{loc}}(\omega)$. At high temperature, ρ_b is centered around $\lambda \sim T \ln[(S+1)/S]$ and $\chi''_{\text{loc}}(\omega)$ is a simple peak. At low temperature, we find in $\chi''_{\text{loc}}(\omega)$ a δ -function peak at zero frequency with weight S^2 , which is associated with longitudinal relaxation (see Ref. 24 for a discussion for $N=2$) and two peaks, centered around $\pm \lambda \propto 1/T$ [cf. Eq. (18)] with a constant width, which are associated with transverse relaxation. Again, these results are very similar to the conclusions reached in Ref. 24 from a fit of the imaginary-time data for $N=2$, using a model $\chi''(\omega)$. The only difference is that the central peak is not broadened by thermal fluctuations in the large- N limit.

Finally, since these solutions describe the formation of a local moment at low temperature and since the onset of the quenching temperature (at which the reduction of the Curie constant sets in) turns out to be lower than the temperature where spin-glass ordering occurs (as shown in the next section), we consider these solutions as a mean-field artifact of the spin-glass ordering. Static limits of such solutions are actually known to occur in the classical SK model. We also note that the internal energy of these solutions has an unphysical divergence as $T \rightarrow 0$.

We close this section by noting that, for small values of the spin S , a rather intricate pattern emerges for the stability and coexistence of the two kinds of paramagnetic solutions described above. We have studied this numerically in some detail, but do not report this here, since most of these phenomena occur below the spin-glass ordering temperature anyway. The important features have been displayed on Fig. 1. We emphasize again that the spin-liquid solutions are the relevant solutions describing the whole quantum-critical regime. Even though they are unstable at $T=0$ for $S > S_{\text{max}}$, they remain consistent *finite-temperature* solutions in a much wider range of values of S for $T < J$. At higher S and above the spin-glass ordering temperature, the paramagnetic phase behaves as a local moment, with the Curie constant getting gradually reduced as T is lowered.

IV. SPIN-GLASS PHASE

In this section, we investigate spin-glass ordering in this model. The first observation that we make (Sec. IV A) is that the spin-glass susceptibility (i.e., the response to a spin-glass ordering field) is actually of order $1/N$ in the large- N limit. This does not preclude a spin-glass phase, but means that the transition is not associated with a linear instability. Indeed, we shall find explicit solutions in the ordered phase in the bosonic case, while the fermionic case does not have a spin-glass phase at $N=\infty$ (but does order as soon as $1/N$ corrections are considered).

A. Spin-glass susceptibility

Here we derive an exact expression for the spin-glass susceptibility, valid for arbitrary N in this mean-field model.

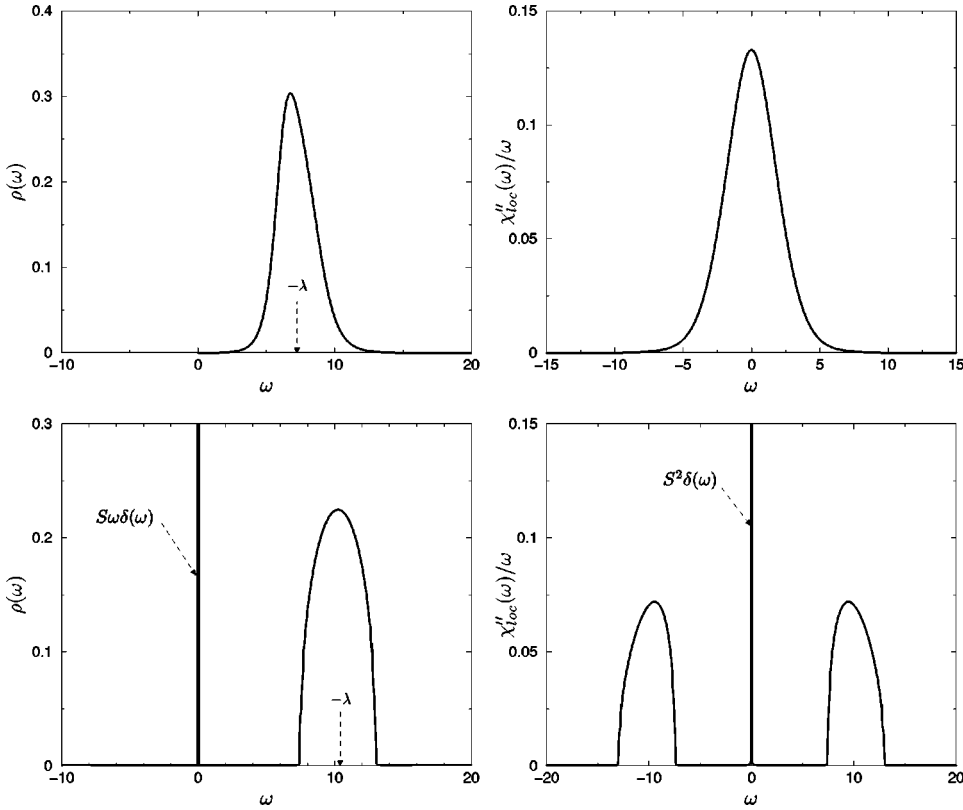


FIG. 5. Spectral densities for G_b (left) and for the local susceptibility χ_{loc} (right), for high temperature (top) and a very low temperature (bottom). These results are extracted from a numerical solution of saddle-point equations (5) in real frequencies.

The derivation is most conveniently performed using replicas. We note that in the presence of spin-glass order, the correlation function $\langle \vec{S}^a(\tau) \cdot \vec{S}^b(\tau') \rangle$ acquires a nonzero value for $a \neq b$, which is, however, static, i.e., independent of $\tau - \tau'$ (see, e.g., Ref. 8). This crucial point is due to the fact that different replicas are independent of one another before averaging, so that, for $a \neq b$,

$$\overline{\langle \vec{S}^a(\tau) \cdot \vec{S}^b(\tau') \rangle} = \overline{\langle \vec{S}^a(\tau) \rangle} \cdot \overline{\langle \vec{S}^b(\tau') \rangle} = \overline{\langle \vec{S}^a(0) \rangle} \cdot \overline{\langle \vec{S}^b(0) \rangle}. \quad (20)$$

In the following, we shall denote by q_{ab} the (normalized) off-diagonal correlation function which is an order parameter for the spin-glass phase:

$$q_{ab} \equiv \frac{1}{N^2} \sum_{a \neq b} \overline{\langle \vec{S}^a(\tau) \cdot \vec{S}^b(\tau') \rangle}. \quad (21)$$

We consider the stability of the paramagnetic phase to this type of ordering and introduce an ordering field H_{ab} conjugate to q_{ab} . This has two effects.

(i) It adds to the effective action (3) an explicit term

$$\delta S = \frac{1}{N} \int d\tau \int d\tau' \sum_{a \neq b} H_{ab} \vec{S}_a(\tau) \cdot \vec{S}_b(\tau'). \quad (22)$$

The normalization of H_{ab} has been chosen in such a way that the change in the total free energy is of order N .

(ii) It modifies the value of the self-consistent field Q^{ab} . The change of the off-diagonal component, to linear order, is imposed by the self-consistency condition (4) to be $\delta Q^{ab} = \delta q_{ab}$, with δq_{ab} the induced order parameter.

One can then perform an expansion of the off-diagonal correlation function up to linear order in both H_{ab} and δQ^{ab} . This yields

$$\delta q_{ab} = \frac{1}{N} \chi_{loc}^2 (H_{ab} + J^2 \delta Q^{ab}), \quad (23)$$

in which χ_{loc} is the local susceptibility of the paramagnetic phase. Since $\delta Q^{ab} = \delta q_{ab}$, this finally yields the susceptibility to spin-glass ordering:

$$\chi_{sg} \equiv \frac{\delta q_{ab}}{H_{ab}} = \frac{1}{N} \frac{\chi_{loc}^2}{1 - (J\chi_{loc})^2/N}. \quad (24)$$

This formula has two important consequences. The susceptibility to spin-glass ordering is of order $1/N$, and any spin-glass instability at $N = \infty$ must be associated with a nonlinear effect of higher order (i.e., come from terms of higher than quadratic order in q_{ab} in the free energy). Furthermore, Eq. (24) shows that for finite N , a (linear) instability into a spin-glass phase will occur when $J\chi_{loc}(T) = \sqrt{N}$. Hence the fermionic model, for which χ_{loc} diverges at low T , will have a spin-glass instability for arbitrary large but finite N . More precisely, since the low-temperature behavior $J\chi_{loc} \sim \ln(J/T)$ has been shown above to hold for all N for the paramagnetic solution of the fermionic case, we conclude from Eq. (24) that the spin-glass transition temperature depends on N in that case as $T_c^f \sim J e^{-\sqrt{N}}$.

B. Spin-glass solutions and the “replicon” problem

We now turn to the explicit construction of solutions of the integral equations (5) with spin-glass ordering, in the bosonic case. The same reasoning as above shows that the Green’s function $G^{ab}(\tau)$ does not depend on τ for $a \neq b$. Thus the most general ansatz for the Green’s function G^{ab} can be written as

$$G^{ab}(\tau) = \begin{cases} \tilde{G}(\tau) - g_1 & (a=b), \\ -g_{ab} & (a \neq b), \end{cases} \quad (25)$$

where $\tilde{G}(\tau)$ is a function of the imaginary time, g_{ab} a constant matrix, and g_1 a constant. By definition, g_1 is fixed so that \tilde{G} is regular at $T=0$, i.e., $\tilde{G}(\tau) \rightarrow 0$ as $\tau \rightarrow \infty$. In the following discussion, we will restrict ourselves to solutions given by a Parisi ansatz for g_{ab} (a replica symmetry breaking scheme). In the $n \rightarrow 0$ limit (where n is the number of replica), this matrix becomes a function $g(u)$ of a continuous variable u with $0 \leq u \leq 1$.²²

Our equations (5) involve the Green function G , whereas the physical quantity is the susceptibility $\chi^{ab}(\tau) = G^{ab}(\tau)G^{ab}(-\tau)$. The order parameter q_{ab} widely introduced in the spin-glass literature²² is given here by $q_{ab} = g_{ab}^2$ or, in the limit $n \rightarrow 0$,

$$q(u) = g(u)^2. \quad (26)$$

The Edwards-Anderson parameter is $q_{EA} = q(1) = g(1)$.^{28,22} Since at zero temperature, in the long-time limit, we find $\lim_{\tau \rightarrow \infty} G^{aa}(\tau)G^{aa}(-\tau) = q_{EA}$, we find $g_1 = g(1)$, by definition of g_1 . More precisely, we look for solutions in which these two definitions of q_{EA} coincide, but it is not really an assumption in our computation: if this relation were violated, we would simply find for \tilde{G} a nonvanishing limit for $\tau \rightarrow \infty$.

Among the various possible replica symmetry breaking schemes,²² we will now focus on *one-step* solutions, since we have not found any other, either two steps or with continuous replica symmetry breaking. In this case, the function $g(u)$ is piecewise constant: $g(u) = \bar{g}$ for $0 < u < x$ and $g(u) = g$ for $x \leq u \leq 1$. In the following, we will refer to x as the *breakpoint*. According to Eqs. (5), the self-energy Σ has the form

$$\Sigma^{ab}(\tau) = \begin{cases} \tilde{\Sigma}(\tau) - J^2 g^3 & (a=b), \\ -J^2 g_{ab}^3 & (a \neq b), \end{cases} \quad (27)$$

with $\tilde{\Sigma}$ is given by Eq. (31b). Using the standard formulas to invert the Parisi matrices in the limit $n \rightarrow 0$,³² we find

$$\tilde{G}^{-1}(i\nu_n) = i\nu_n + \lambda - \tilde{\Sigma}(i\nu_n), \quad (28)$$

$$J^2 g^2 \tilde{G}(i\nu_n = 0)^2 = 1 + J^2 \beta x g^3 \tilde{G}(i\nu_n = 0). \quad (29)$$

At this stage, it is useful to introduce here a new parameter Θ defined by

$$\tilde{G}(i\nu_n) = -\frac{\Theta}{Jg}. \quad (30)$$

We then eliminate λ in Eq. (28) and $\tilde{G}(0)$ in Eq. (29) and obtain finally a closed set of equations for \tilde{G} and g :

$$[\tilde{G}(i\nu_n)]^{-1} = i\nu_n - \frac{Jg}{\Theta} - [\tilde{\Sigma}(i\nu_n) - \tilde{\Sigma}(0)], \quad (31a)$$

$$\begin{aligned} \tilde{\Sigma}(\tau) = J^2 [& \tilde{G}^2(\tau)\tilde{G}(-\tau) - 2g\tilde{G}(\tau)\tilde{G}(-\tau) - g\tilde{G}^2(\tau) \\ & + 2g^2\tilde{G}(\tau) + g^2\tilde{G}(-\tau)], \end{aligned} \quad (31b)$$

$$\tilde{G}(\tau = 0^-) = -(S - g), \quad (31c)$$

$$\beta x = \frac{1}{Jg^2} \left(\frac{1}{\Theta} - \Theta \right). \quad (31d)$$

The crucial observation at this point is that these saddle-point equations possess a one-parameter family of solutions, parametrized by Θ or equivalently by the breakpoint x . This phenomenon already occurs in other models which have a *one-step* replica symmetry breaking solution.³³ The determination of the breakpoint turns out to be the most difficult question of this analysis. Two possible criteria are the following.

(1) To minimize the free energy $\mathcal{F}(x)$ as a function of x , as would be required by the thermodynamics. In the following, we will refer to this as the *equilibrium criterion*. This criterion has been used in a previous attempt to understand this spin-glass phase.²³

(2) To impose a vanishing lowest eigenvalue of the fluctuation matrix in the replica space. We will refer to this as the *marginality* or *replicon* criterion. Although it is not really justified up to now, we will argue that it is the correct choice.

This problem is not due to the quantum aspect of our model: it already appears similarly in some classical spin-glass models, in the p -spin model, for example. In this classical model, the study of the dynamics shows the existence of a dynamical transition T^{dyn} above the static spin-glass temperature T^{eq} given by the static solution of the mean-field model. It turns out that, in this classical model, the replicon criterion has been proven to give the same transition temperature $T^c = T^{\text{dyn}}$. Moreover, it has been shown^{34,35} that the same phenomenon occurs in some *quantum* version of the p -spin model. Thus, using this condition, it is possible in some sense to mimic the dynamics by simply solving a static problem, although this is not fully understood at present.

In the present model, the two criteria give a coherent solution, but with totally different spectra of *equilibrium* fluctuations: the equilibrium criterion leads to a gap in $\chi''(\omega)$, whereas the replicon criterion is the only one which gives a *gapless* $\chi''(\omega)$ (a similar observation was made in Ref. 33 in a one-dimensional quantum model with disorder). We believe that in this quantum Heisenberg spin glass the replicon criterion provides us with the correct physical solution (T_c), contrary to the equilibrium solution, which gives the static transition temperature (T_{eq}). However, this claim cannot be proved in the present context: in particular, the static solution does give a full solution of Eqs. (5). A study of the true Hamiltonian dynamics in real time and finite temperature of this quantum problem is necessary for a deeper understand-

ing of this question, but this is beyond the scope of this paper. Let us now examine the two criteria separately in more detail.

1. Replicon criterion

To apply the replicon criterion, we need to study the fluctuations of the free energy in the replica space around the one-step solution. In the large- N limit, the free energy is given by the expression

$$\begin{aligned} \mathcal{F}[G^{ab}, \lambda] = & \frac{1}{\beta} \sum_n \text{Tr} \ln [i\nu_n + \lambda - \Sigma^{ab}(i\nu_n)] \\ & + \frac{3J^2}{4} \sum_{ab} \int_0^\beta d\tau [G^{ab}(\tau)G^{ab}(-\tau)]^2 - \lambda S. \end{aligned} \quad (32)$$

Under infinitesimal variation δg_{ab} for $a \neq b$, the variation of the free energy is (up to second order)

$$\delta \mathcal{F} = \sum_{\substack{a>b \\ c>d}} M_{ab,cd} \delta g_{ab} \delta g_{cd}. \quad (33)$$

Strictly speaking, as this is a quantum problem, we have to simultaneously consider the variation of the diagonal component, $\delta \tilde{G}(\tau)$ in Eq. (25), in a study of the fluctuations. In a spin-glass phase, there is indeed a coupling between δg_{ab} and $\delta \tilde{G}(\tau)$ which modifies the fluctuation eigenvalues. Fortunately, however, as we show in Appendix B, this coupling does not modify the eigenvalue e_1 and our main result (35) below, and so we will neglect $\delta \tilde{G}(\tau)$ here. The diagonalization of the $n(n-1)/2 \times n(n-1)/2$ matrix M is briefly explained in Appendix B and gives three eigenvalues

$$\begin{aligned} e_1 &= 3\beta J^2 g^2 (1 - 3\Theta^2), \\ e_2 &= \frac{3\beta J^2 g^2}{\Theta^2} [\Theta^2 - 3 + 3\beta J g^2 \Theta (1 + \Theta)], \\ e_3 &= 6\beta J^2 g^2 (3\beta J g^2 \Theta - 1). \end{aligned} \quad (34)$$

A first consequence of this analysis is that replica-symmetric solutions are unstable, since from Eq. (31d) they correspond to $\theta=1$ and then $e_1 < 0$. Hence these solutions will not be considered in the following discussion.

A full solution of Eqs. (34) is required to show the positivity of e_2, e_3 , but we immediately see that $e_1 = 0$ for

$$\Theta_R = \frac{1}{\sqrt{3}}. \quad (35)$$

Quite remarkably, we will see below in Sec. IV C 2 and Appendix B 2 that precisely the same value of Θ is selected by a criterion which is seemingly entirely independent. We will study the dynamic spectral functions in the spin-glass phase as defined by $\tilde{G}(\tau)$, and show that their associated spectral densities are nonzero as $|\omega| \rightarrow 0$ only for the value of Θ in Eq. (35). So marginal stability in replica space appears

to be connected to a gapless quantum excitation spectrum. We may intuitively understand this as due to the availability of many low-energy states when the system first freezes, but a better understand should emerge from a real-time analysis.

2. Equilibrium criterion

To apply the equilibrium criterion, we start from the expression of the free energy \mathcal{F} and solve for x :

$$\frac{d\mathcal{F}(x)}{dx} = 0. \quad (36)$$

The computation of the *total* derivative (36) reduces to $\partial_x \mathcal{F}(x)|_{\tilde{G}, \lambda}$ because the saddle-point equations (5) for *finite* n are equivalent to

$$\frac{\partial \mathcal{F}}{\partial G^{ab}} = \frac{\partial \mathcal{F}}{\partial \lambda} = 0 \quad (37)$$

as can be checked by an explicit calculation. Computing the logarithm in Eq. (32) (using Appendix II of Ref. 32) and taking the derivative leads to

$$\frac{3}{4} J^2 g^4 - \frac{2}{(\beta x)^2} \ln[-Jg\tilde{G}(i\nu_n=0)] = - \frac{g}{\beta x \tilde{G}(i\nu_n=0)} \quad (38)$$

and finally to an equation for Θ :

$$2 \ln \Theta + \frac{1}{4\Theta^2} + \frac{1}{2} - \frac{3\Theta^2}{4} = 0. \quad (39)$$

This equation has two solutions: the replica-symmetric one $\Theta = 1$ (unstable, as explained above) and a nontrivial one $\Theta = \Theta_{\text{eq}} \approx 0.4421 \dots$. Contrary to the previous solution, we will see in Sec. IV C 2 that $\text{Im} \tilde{G}$ has a gap for this value of Θ .

C. Phase diagram

Once Θ has been determined, Eqs. (31) can be solved either numerically (both in imaginary time and in real frequency) or analytically in the $S \rightarrow \infty$ limit. In the following, we will mainly restrict ourselves to $\Theta = \Theta_R$ since we believe that it is the correct solution. However, all calculations have been redone for $\Theta = \Theta_{\text{eq}}$ with related results.

1. Numerical solution

First, the critical temperature is obtained from the numerical solution of Eqs. (31) in imaginary time: the spin-glass order parameter $q(T) = g^2(T)$ and the breakpoint $x(T)$ are displayed in Fig. 6 as a function of the temperature. x increases linearly with T from 0 at $T=0$ (there is no replica symmetry breaking at zero temperature), and T_{sg} is determined by the condition $x(T_{\text{sg}}) = 1$, since we must have $0 \leq x \leq 1$ by definition.²² Hence there is a discontinuity in q at the transition, but we will show below that the transition is second order. A careful numerical study shows that the transition is always driven by $x=1$ for all values of S and produces the critical temperature displayed in Fig. 1. The com-

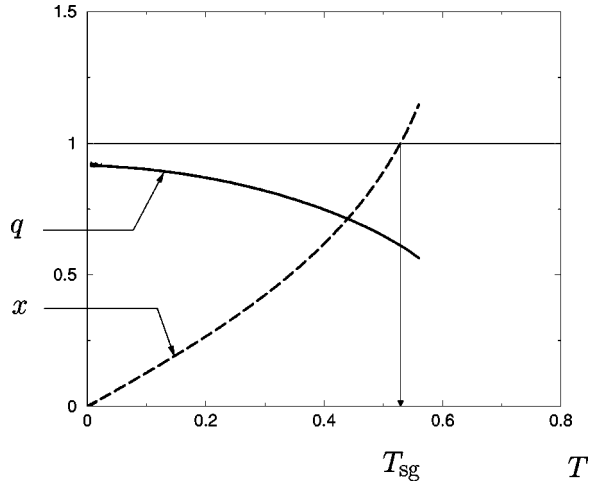


FIG. 6. The Edwards-Anderson parameter q_{EA} and the breakpoint x as a function of the temperature T for a fixed value of the size of the spin $S=1$ ($J=1$). The transition to the paramagnet is given by the condition $x=1$.

putation is similar for the critical temperature T_{sg}^c given by the ‘‘replicon’’ criterion and for the critical temperature $T_{\text{sg}}^{\text{eq}}$ given by the equilibrium criterion. Moreover, we find that T_{sg}^c , the *dynamic* transition temperature, is higher than $T_{\text{sg}}^{\text{eq}}$, the *static* transition temperature: this is required by our physical interpretation of the two solutions, but it was not obvious *a priori* from the integral equations solved.

2. Large- S limit and spectral densities

Further analytical insight into the spin-glass phase itself can be obtained by considering various large- S limits, which differ by the manner in which temperatures and frequencies are scaled with S (see Fig. 1).

In a first simple large- S limit, we take T large enough so that $T/J S^2$ is of order unity. This is the simple classical limit in which we can neglect all nonzero Matsubara frequencies and Eq. (1) reduces to the classical problem in which \vec{S} are

commuting vectors of length S . Equations (5) are analytically solvable, and we can obtain a closed-form expression for the critical temperature at which spin-glass order vanishes:

$$T_{\text{sg}}^c \sim \frac{2}{3\sqrt{3}} J S^2. \quad (40)$$

A second, more sophisticated limit, valid at lower temperatures (well within the spin-glass phase), is when we examine ω and T of order $J S$. It is therefore useful to define the variables $\bar{\omega} = \omega/(J S)$ and $\bar{T} = T/(J S)$, which remain of order unity at large S . With this scaling, the integral equations (31) reduce to independent quartic equations for each frequency. More precisely, if we make the following ansatz for the Green’s function,

$$\tilde{G}(\omega, T) = \frac{1}{J S} g_1(\bar{\omega}, \bar{T}) + \frac{1}{J S^2} g_2(\bar{\omega}, \bar{T}) + \dots, \quad (41)$$

then to leading order in $1/S$, Eqs. (31) reduce to

$$g(T) = S - \int_{-\infty}^{\infty} \rho_1(\bar{\omega}) d\bar{\omega},$$

$$g_1(\bar{\omega})^{-1} = \bar{\omega} - \frac{1}{\Theta} - 3\Theta - 2g_1(\bar{\omega}) - \overline{g_1(-\bar{\omega})}, \quad (42)$$

where $\rho_1 = -\text{Im} g_1/\pi$ as usual. Eliminating the frequency $-\bar{\omega}$, we find a quartic equation for $g_1(\bar{\omega})$. We do not explicitly display the far more complicated equation for the subleading term g_2 .

The solution of the quartic equation for $\Theta = \Theta_R$ is presented on Fig. 7 together with a numerical solution of the full integral equation for $S=5$. From the solution of the quartic equation, we find that ρ_1 vanishes linearly frequency at low frequencies; indeed, we find the analytic expansion

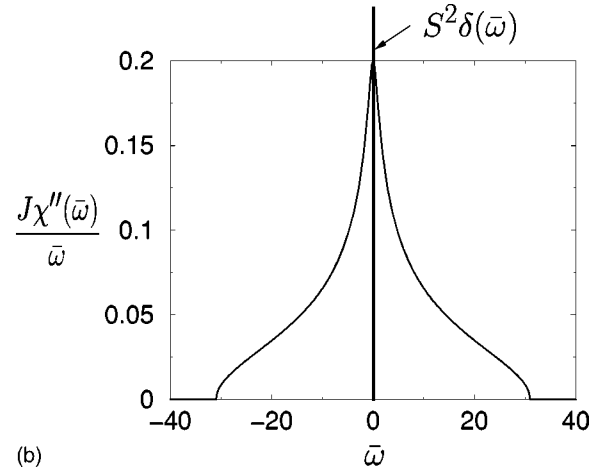
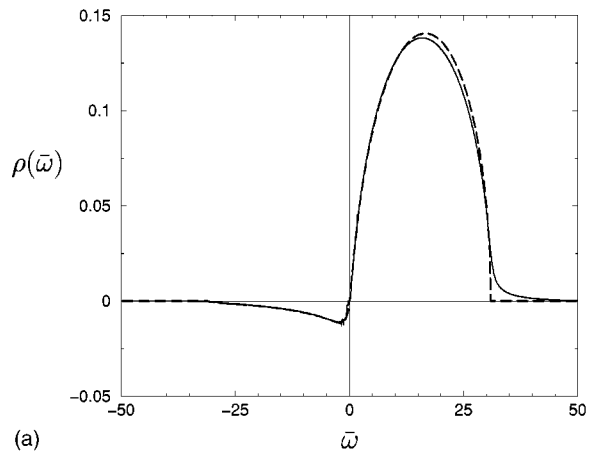


FIG. 7. (a) $\rho_1(\omega)$ at $T \approx 0$ for $S=5$ and $\Theta = \Theta_R$: the solid line is the numerical solution for the integral equation (31); the dashed line is the solution of the quartic equation (41) for g_1 . (b) $\chi''(\omega)/\omega$ at $T \approx 0$ from the quartic equation.

$$g_1(\bar{\omega}) = -\frac{1}{\sqrt{3}} - \frac{(1+i)}{2} \bar{\omega} + \frac{(2-3i)\sqrt{3}}{4} \bar{\omega}^2 \quad (43)$$

at low frequencies. We expect that the full Green's function in Eq. (41) also has a similar low-frequency expansion, although this has not been proved. It is not difficult to show that the linear low-frequency spectral density holds at higher orders in the $1/S$ expansion; moreover, our numerical results, shown in Fig. 7, also clearly indicate a linear behavior at small ω . At dominant order in the present large- S theory, the spin susceptibility is given by

$$\begin{aligned} \chi''(\omega) = & -\pi \int_0^\omega dx \rho_1(x) \rho_1(x-\omega) + g \pi [\rho_1(\omega) - \rho_1(-\omega)] \\ & + \pi g^2 \beta \omega \delta(\omega) \end{aligned} \quad (44)$$

and this is also shown in Fig. 7.

It is important to realize that the deceptively simple structure in Eq. (43) relies on the special value $\Theta = \Theta_R = 1/\sqrt{3}$ determined by the entirely different replicon argument in Sec. IV B 1. For arbitrary values of Θ , we find either no physically sensible solution of the large- S quartic equation (this is the case at the replica symmetric value $\Theta = 1$ where the spectral density does not satisfy the required positivity criteria) or a solution with a spectral gap. In the latter case, the solution for g_1 is real for small real $\bar{\omega}$, and there is an onset in the imaginary part $\sim (\bar{\omega} - \bar{\omega}_c)^{1/2}$ above some critical frequency $\bar{\omega}_c$. The solution for $\Theta = \Theta_{eq}$ is of the second type: it has a finite-energy gap, but does not violate any spectral positivity criteria.

This subsection has so far identified two distinct large- S regimes. In the regime $T \sim JS^2$, we have purely classical behavior (the nonzero Matsubara frequencies can be neglected for static properties) and a phase transition at a critical temperature in Eq. (40) where the spin-glass order vanishes. At lower temperatures $T \sim JS$, we are well within the spin-glass phase, and the semiclassical dynamics is described

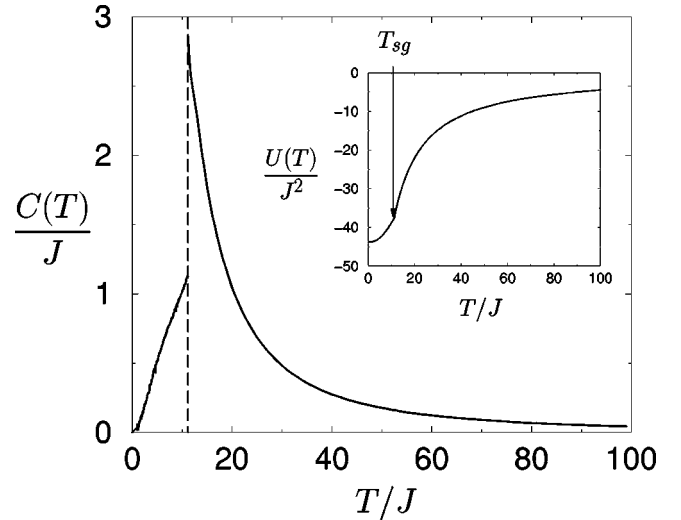


FIG. 8. The specific heat $C(T)$ and the internal energy $U(T)$ vs the temperature T , from a numerical solution of Eqs. (31) for $S = 5$ and $\Theta = \Theta_R$.

by the solution of a quartic equation defined by Eq. (42). As we noted in Fig. 1, there is a third “quantum” regime at even lower temperatures $T \sim J\sqrt{S}$, and this becomes evident in a study of the thermodynamic properties presented in the following section.

D. Thermodynamics

We now turn to the internal energy U and the specific heat C . By computing the average of the Hamiltonian in the $N \rightarrow \infty$ limit, we find that U is given by

$$U(T) = -\frac{J^2}{2} \int_0^\beta d\tau [G^{ab}(\tau)G^{ab}(-\tau)]^2. \quad (45)$$

Using Eq. (25) and the one-step replica symmetry breaking ansatz in the spin-glass phase, we find

$$U(T) = \begin{cases} -\frac{J^2}{2} \int_0^\beta G(\tau)^2 G(-\tau)^2 d\tau & \text{in the paramagnetic phase} \\ -\frac{J^2}{2} \int_0^\beta [G(\tau) - g]^2 [G(-\tau) - g]^2 d\tau - \frac{J^2}{2} \beta (x-1) g^4 & \text{in the spin glass phase.} \end{cases} \quad (46)$$

A numerical computation of the internal energy $U(T)$ and the specific heat $C(T)$ is displayed in Fig. 8 for $\Theta = \Theta_R$. The condition for the phase transition between the two phases is that the breakpoint in the Parisi function reach its limiting value $x=1$. In this limit the equations determining the parameters in the spin-glass phase, Eqs. (31), transform continuously to those for the paramagnet. As the equations are

believed to have a unique solution, this implies that there is no discontinuity in the internal energy at the transition, indicating its second-order nature. This is confirmed by the numerical solution displayed in Fig. 8.

Moreover, in the large- S limit defined above, we can perform a low-temperature expansion of the internal energy. Inserting Eqs. (41) and (42) into Eq. (45), and keeping the

dominant terms at large S , we find

$$\begin{aligned}
U(T) &= -\frac{J}{2} \left(\frac{1}{\Theta} + 3\Theta \right) g^2 - J^2 g^2 \frac{1}{\beta} \sum_{\nu_n} \\
&\quad \times [\tilde{G}(i\nu_n) \tilde{G}(-i\nu_n) + 2\tilde{G}^2(i\nu_n)] + \dots \\
&= -\frac{JS^2}{2} \left(\frac{1}{\Theta} + 3\Theta \right) + JS \left(\frac{1}{\Theta} + 3\Theta \right) \bar{T} \sum_{\bar{\nu}_n} g_1(i\bar{\nu}_n) \\
&\quad - JS \bar{T} \sum_{\bar{\nu}_n} [g_1(i\bar{\nu}_n) g_1(-i\bar{\nu}_n) + 2g_1^2(i\bar{\nu}_n)] + \mathcal{O}(JS^0),
\end{aligned} \tag{47}$$

where $\bar{\nu}_n = \nu_n / (JS)$. Clearly, this result indicates that the leading term in $U(T)$ is a temperature-independent constant of order JS^2 , followed by a term of order JS whose coefficient is a function only of (T/JS) . Evaluation of the latter function at low T for $\Theta = \Theta_R$ yields a curious accident: the gapless structure of the spectral functions suggests that the low- T expansion should depend only on even powers of T/JS , but it is not difficult to show using Eq. (43) that the coefficient of the term of order $S(T/JS)^2$ vanishes. The first nonvanishing, T -dependent term among those shown explicitly in Eq. (47) turns out to be order $JS(T/JS)^4$. To obtain the true low- T behavior, we need to expand Eq. (47) to one higher order in $1/S$, and this requires use of the second term, g_2 , in Eq. (41). We do not expect any cancellation of the term of order $(T/JS)^2$ at this point, and so the low- T expansion for U looks like

$$U(T) = U(0) + aS(T/JS)^4 + b(T/JS)^2 + \dots \tag{48}$$

Rather than numerically evaluating the values a and b , we will be satisfied by the full numerical solution of Eqs. (31), followed by the evaluation of Eq. (46). The results are shown in Fig. 8 and are consistent with Eq. (48). The structure of the expansion in Eq. (48) suggests that these results are valid for $T < J\sqrt{S}$, where the specific heat depends linearly on the temperature. Although the present discussion has been carried out for large S , we expect—and this is supported by our numerical results—that the linear T dependence of the specific heat holds even for small S as $T \rightarrow 0$.

In Appendix C we describe the computation of the specific heat of the quantum rotor and Ising spin glasses considered in Ref. 13. As noted in the Introduction, these models are simpler because they do not have quantum Berry phases in their effective action. Further, at low orders in their Landau theory, the solution for the spin-glass phase is replica symmetric. However, understanding the true $T \rightarrow 0$ behavior requires inclusion of higher-order, “dangerously irrelevant” terms which induce replica symmetry breaking; this is carried out in Appendix C, and we find that these quantum spin glasses also have a linear specific heat at low T .

V. CONCLUSION

We believe that the results of this paper provide a reasonably complete understanding of the infinite-range quantum Heisenberg spin glass. While there have been a large number

of previous studies of quantum spin glasses of Ising spins and rotors [including models with $(p > 2)$ -spin interactions], none of these models contain quantum Berry phases in their effective actions, as is the case with the Heisenberg model. They have strong consequences: the spin-liquid solution of Sec. II A and its spectral density (9) are novel properties of the Heisenberg model. There is an intricate interplay in stability between this spin-liquid state and the state with spin-glass order at low T , which we have also described. At sufficiently low T , the spin-glass order always appears, and we have also described the thermodynamic properties of this state.

An important issue not resolved in our analysis is the origin of the marginal stability criterion in the fluctuation eigenvalues in replica space. We imposed this criterion in a rather *ad hoc* manner and found that it was the unique case under which the quantum excitation spectrum was gapless. Ultimately, the selection criterion for the spin-glass state has to be a dynamic one, and this requires an analysis of the approach to equilibrium in real-time dynamics. Such an analysis was not carried out here and is an important direction for future research.

Another interesting open problem is to extend the study of Eq. (1) to cases where J_{ij} has a nonzero average value. This will allow for ground states with other types of magnetic order, ferromagnetic and antiferromagnetic, and their competition with the spin-glass state should be of some experimental interest. Interesting transitions in the paramagnetic states from the spin-liquid state discussed also appear possible.

We have already mentioned a recent study²⁵ of the quenching of the spin-liquid state by mobile charge carriers into a disordered Fermi liquid. Combining this with models just mentioned, with a nonzero average J_{ij} , should lead to results of direct physical interest in the heavy fermion and cuprate series of compounds.

ACKNOWLEDGMENTS

We thank G. Biroli, L. Cugliandolo, D. Grempel, P. Le Doussal, and M. Rozenberg for useful discussions. S.S. was supported by U.S. NSF Grant No. DMR 96-23181. O.P. was supported by the Center of Material Theory, Rutgers University.

APPENDIX A: COMPUTATION OF THE SPECTRAL ASYMMETRY

This appendix is devoted to the derivation of Eqs. (10). We will consider hereafter the fermionic case (the bosonic one is very similar). At zero temperature, the number of particles is given by

$$\begin{aligned}
q_0 &= i \int_{-\infty}^{\infty} \frac{d\omega}{2\pi} G_f^F(\omega) e^{i\omega 0^+} \\
&= iP \int_{-\infty}^{\infty} \frac{d\omega}{2\pi} \partial_\omega \ln G_f^F(\omega) e^{i\omega 0^+} \\
&\quad - iP \int_{-\infty}^{\infty} \frac{d\omega}{2\pi} G_f^F(\omega) \partial_\omega \Sigma_f^F(\omega) e^{i\omega 0^+}
\end{aligned} \tag{A1}$$

where G^F is the Green's function with Feynman prescription on the real axis and the symmetric principal part is defined by

$$P \int_{-\infty}^{\infty} = \lim_{\eta \rightarrow 0} \int_{-\infty}^{-\eta} + \int_{\eta}^{\infty}. \quad (\text{A2})$$

Using the relation between G^F and the *retarded Green's function* G^R , we find, for the first term,

$$\begin{aligned} iP \int_{-\infty}^{\infty} \frac{d\omega}{2\pi} \partial_{\omega} \ln G_f^F(\omega) e^{i\omega 0^+} \\ = \frac{\arg G_f^R(0^-) - \arg G_f^R(-\infty)}{\pi} \\ + iP \int_{-\infty}^{\infty} \frac{d\omega}{2\pi} \partial_{\omega} \ln G_f^R(\omega) e^{i\omega 0^+}. \end{aligned} \quad (\text{A3})$$

The arguments can be extracted from the low- and high-energy behavior of the Green's function, which leads to $\arg G_f^R(0^-) = -3\pi/4 - \theta$ and $\arg G_f^R(-\infty) = -\pi$, respectively. The integral on the right of Eq. (A3) can be easily evaluated: we close the contour of integration, avoiding the singularity at $\omega = 0$, and use the analyticity of the retarded Green's function in the upper half plane, in which it has no zeros or poles. We find, finally,

$$q_0 = \frac{1}{2} - \frac{\theta}{\pi} - iP \int_{-\infty}^{\infty} \frac{d\omega}{2\pi} G_f^F(\omega) \partial_{\omega} \Sigma_f^F(\omega) e^{i\omega 0^+}. \quad (\text{A4})$$

The problem is now reduced to the computation of the integral in Eq. (A4) as function of θ , which turns out to be the most difficult point. An analogous computation was performed in the overscreened regime of a large- N description of Kondo effects,^{26,27} but it turns out to be more complex here. Proceeding along the lines of Refs. 26 and 27, we note the existence of the Luttinger-Ward functional $\Phi_{\text{LW}} = \int dt G^2(t) G^2(-t)$, which has two properties: first, we have $\Sigma^R(\omega) = \delta \Phi_{\text{LW}} / \delta G^R(\omega)$; second Φ_{LW} is invariant in the transformation $G(\omega) \rightarrow G(\omega + \epsilon)$. From this, we could naively think that the integral of Eq. (A4) vanishes. However, it is not possible to find a regularization for the integral for which we could use the invariance of the Luttinger-Ward functional and a more careful analysis shows that

$$iP \int_{-\infty}^{\infty} \frac{d\omega}{2\pi} G_f^F(\omega) \partial_{\omega} \Sigma_f^F(\omega) = \frac{\sin 2\theta}{4}. \quad (\text{A5})$$

To obtain this result, we introduce the following parametrization of the singularity at $\omega = 0$:

$$\rho(\omega) \sim \begin{cases} \frac{C_+}{\sqrt{\omega}} & \text{for } \omega > 0, \\ \frac{C_-}{\sqrt{|\omega|}} & \text{for } \omega < 0. \end{cases} \quad (\text{A6})$$

The principle of the computation is very simple: we compute explicitly the integral with a regulator $\eta > 0$ and then perform the limit $\eta \rightarrow 0$. Going to the real axis, we find

$$\begin{aligned} \Sigma^F(\omega) = - \int_{\substack{\omega_1 > 0 \\ \omega_2 > 0 \\ \omega_3 < 0}} \int_{\substack{\omega_1 < 0 \\ \omega_2 < 0 \\ \omega_3 > 0}} d\omega_1 d\omega_2 d\omega_3 \\ \times \frac{\rho(\omega_1)\rho(\omega_2)\rho(\omega_3)}{\omega_1 + \omega_2 - \omega_3 - \omega - i0^+ \text{sgn } \omega_1}. \end{aligned} \quad (\text{A7})$$

Using the notation $a = \bar{a} + i\epsilon_a$, $b = \bar{b} + i\epsilon_b$, $\epsilon_{a/b} = \pm 0^+$, and $\psi_{\eta}(x) = \Theta(|x| - \eta)$ (\bar{a} are \bar{b} real and Θ is the Heaviside function), we obtain [using the definition of the principal part (A2)]

$$\begin{aligned} \phi_{\eta}(a, b) = P \int_{-\infty}^{\infty} \frac{dz}{(z-a)^2(z-b)} \\ = \frac{1}{(a-b)^2} \left(\ln \left| \frac{(\eta+b)(\eta-a)}{(\eta-b)(\eta+a)} \right| \right. \\ \left. + i\pi\psi_{\eta}(b)\text{sgn } \epsilon_b - i\pi\psi_{\eta}(a)\text{sgn } \epsilon_a \right) \\ + \frac{1}{a-b} \left(\frac{1}{\eta-a} + \frac{1}{\eta+a} \right). \end{aligned} \quad (\text{A8})$$

Using the spectral representation for G^F and Eq. (A7), we find

$$\begin{aligned} \mathcal{I} = - \int_{\Delta_2 \cup \Delta_2} \prod_{k=0}^3 d\omega_k \rho(\omega_0)\rho(\omega_1)\rho(\omega_2)\rho(\omega_3) \phi_{\eta} \\ \times (\omega_1 + \omega_2 - \omega_3 - i\epsilon_1 \text{sgn } \omega_1, \omega_0 - i\epsilon_0 \text{sgn } \omega_0) \end{aligned} \quad (\text{A9})$$

with an explicit integration over ω with Eq. (A8). In this expression, the integration domains are defined as

$$\begin{aligned} \Delta_1 = \left\{ \begin{array}{l} \omega_0 < 0 \\ \omega_1 > 0 \\ \omega_2 > 0 \\ \omega_3 < 0 \end{array} \right\} \cup \left\{ \begin{array}{l} \omega_0 > 0 \\ \omega_1 < 0 \\ \omega_2 < 0 \\ \omega_3 > 0 \end{array} \right\}, \\ \Delta_2 = \left\{ \begin{array}{l} \omega_0 > 0 \\ \omega_1 > 0 \\ \omega_2 > 0 \\ \omega_3 < 0 \end{array} \right\} \cup \left\{ \begin{array}{l} \omega_0 < 0 \\ \omega_1 < 0 \\ \omega_2 < 0 \\ \omega_3 > 0 \end{array} \right\}. \end{aligned} \quad (\text{A10})$$

Since $\phi_{\eta}(-a, -b) = -\phi_{\eta}(a, b)$, a simple change of variable leads to

$$\begin{aligned} \mathcal{I} = - \int_{x_i > 0} \{ [\rho(\omega_1)\rho(\omega_2)\check{\rho}(\omega_3)\check{\rho}(\omega_0) \\ - \check{\rho}(\omega_1)\check{\rho}(\omega_2)\rho(\omega_3)\rho(\omega_0)] \phi_{\eta} \\ \times (x_1 + x_2 + x_3 - i\epsilon_1, -x_0 + i\epsilon_0) \end{aligned}$$

$$\begin{aligned}
& + [\rho(\omega_1)\rho(\omega_2)\check{\rho}(\omega_3)\rho(\omega_0) \\
& - \check{\rho}(\omega_1)\check{\rho}(\omega_2)\rho(\omega_3)\check{\rho}(\omega_0)]\phi_\eta \\
& \times (x_1+x_2+x_3-i\epsilon_1, x_0-i\epsilon_0)\}, \quad (\text{A11})
\end{aligned}$$

with $\check{\rho}(\omega) = \rho(-\omega)$. To take the limit $\eta \rightarrow 0$, we use the new variables $x_i = \eta u_i$ and the behavior of $\rho(x)$ for $x \rightarrow 0$, parametrized according to Eq. (A6). The first integral in Eq. (A11) vanishes at dominant order in η (this term is proportional to $C_+^2 C_-^2 - C_-^2 C_+^2 = 0$), but the second integral gives

$$\begin{aligned}
\mathcal{I} = & \int_{u_i > 0} \frac{C_+^3 C_- - C_-^3 C_+}{\sqrt{u_0 u_1 u_2 u_3}} \phi_{\eta=1} \\
& \times (u_1 + u_2 + u_3 - i\epsilon_1, u_0 - i\epsilon_0). \quad (\text{A12})
\end{aligned}$$

Using $x = u_0$, $y = u_1 + u_2 + u_3$, and polar coordinates in $\sqrt{u_i}$, we find $\mathcal{I} = 2\pi(C_+^3 C_- - C_-^3 C_+)\mathcal{I}_2$ with

$$\begin{aligned}
\mathcal{I}_2 = & \int_0^\infty \int_0^\infty \frac{dx}{\sqrt{x}} \sqrt{y} dy \left[\frac{1}{(x-y+i\epsilon)^2} \right. \\
& \times \left(\ln \left| \frac{1+x}{1-x} \frac{1-y}{1+y} \right| + i\pi[\psi_1(y) - \psi_1(x)] \right) \\
& \left. + \frac{1}{y-x-i\epsilon} \left(\frac{1}{1-y+i\epsilon_1} + \frac{1}{1+y-i\epsilon_1} \right) \right]. \quad (\text{A13})
\end{aligned}$$

After an integration by parts on y and using

$$\int_0^1 \frac{dx}{x} \ln \left| \frac{1+x}{1-x} \right| = \frac{\pi^2}{4} \quad (\text{A14})$$

we find

$$iP \int_{-\infty}^\infty \frac{d\omega}{2\pi} G_f^F(\omega) \partial_\omega \Sigma_f^F(\omega) = \frac{\pi^3}{2} (C_+^3 C_- - C_-^3 C_+). \quad (\text{A15})$$

Finally, an analogous computation can be performed in the bosonic case, leading in both cases to

$$iP \int_{-\infty}^\infty \frac{d\omega}{2\pi} G^F(\omega) \partial_\omega \Sigma^F(\omega) = \frac{\sin 2\theta}{4} \quad (\text{A16})$$

(in this expression, $-\pi \leq \theta \leq \pi$). These expressions have been shown to agree perfectly with numerical computations in imaginary time for the fermionic case and on the real axis at zero temperature in the bosonic case.

Let us note finally that we can guess the result if we admit *a priori* that the integral is given by an homogeneous polynomial of degree 4: due to the particle-hole symmetry (in the fermionic case $f \leftrightarrow f^\dagger$, the result can be expressed as a function of $C_+^4 - C_-^4$ and $C_+^3 C_- - C_-^3 C_+$). The first term is rejected since it leads to a singularity at $\theta = \pm \pi/4$. The proportionality coefficient is fixed by imposing $\theta = \pi/4$ for $q_0 = 0$.

APPENDIX B: THE MARGINALITY CRITERION

1. Diagonalization of the fluctuation matrix

First, we diagonalize the fluctuation matrix M in the replica space defined by Eq. (33). *A priori* M is a $n(n-1)/2 \times n(n-1)/2$ matrix. However, we have taken for g_{ab} the simple one-step replica symmetry breaking ansatz on g_{ab} ; i.e., the $n \times n$ matrix splits into $n/m \times n/m$ blocks: $g_{ab} = g$ if $[a/m] = [b/m]$, 0 otherwise. Thus M splits into n/m identical $m(m-1)/2 \times m(m-1)/2$ blocks ($M_{ab,cd}$ does not vanish if and only if all indices are in the same block $[a/m] = [b/m] = [c/m] = [d/m]$). Hence the diagonalization is to be performed only on one block (we set $1 \leq a, b, c, d \leq m$), which elements are given by (with a, b, c, d distinct replica indices)

$$M_{ab,ab} = A \equiv 3\beta J^2 g^2 \left\{ 1 - 3\beta^2 J^2 g^2 \left[g^2 + \left(g + \frac{\Theta}{\beta J g} \right)^2 \right] \right\}, \quad (\text{B1})$$

$$M_{ab,ac} = B \equiv -9\beta^3 J^4 g^5 \left(2g + \frac{\Theta}{\beta J g} \right), \quad (\text{B2})$$

$$M_{ab,cd} = C \equiv -18\beta^3 J^4 g^6. \quad (\text{B3})$$

This matrix has already been diagonalized in Ref. 36 and its eigenvalues are given by

$$e_1 = A - 2B + C. \quad (\text{B4})$$

$$e_2 = A + 2(m-2)B + (m-2)(m-3)C/2. \quad (\text{B5})$$

$$e_3 = A + (m-4)B - (m-3)C. \quad (\text{B6})$$

Moreover, the degeneracies of e_1 , e_2 , and e_3 are $n(m-3)/2$, n/m , and $n(m-1)/m$, respectively. Using Eqs. (B1) and (B4), we find finally the result of the text, Eq. (34).

The above calculation has entirely ignored perturbations $\delta\tilde{G}(\tau)$ in the diagonal elements of Eq. (25). Including these greatly complicates the analysis, but a simple observation will suffice for our purposes. Our main attention is on the cross-coupling between $\delta\tilde{G}(\tau)$ and the δg_{ab} . A simple consequence of the block-diagonal structure of the g_{ab} in the mean-field solution is that this cross-coupling has the form

$$\delta\mathcal{F} \sim \sum_{a>b, [a/m]=[b/m]} \int_0^\beta d\tau \delta\tilde{G}(\tau) \delta g_{ab}. \quad (\text{B7})$$

Now we can expand δg_{ab} in terms of the eigenvectors associated with Eq. (B4), which were computed in Ref. 36. The key observation is that after the sum over a, b in Eq. (B7), the cross-terms corresponding to all the eigenvectors associated with e_1 vanish. Consequently, these eigenvectors remain eigenvectors even upon including $\delta\tilde{G}(\tau)$, and the eigenvalue e_1 remains unchanged. A similar argument shows that the eigenvalue e_3 also remains unchanged, and only the eigenvectors associated with e_2 are modified nontrivially by the coupling to $\delta\tilde{G}(\tau)$.

2. Replica solution is gapless

Let us assume that there is no gap in the boson spectral density and more precisely that for small ω :

$$\begin{aligned} \tilde{G}(\omega) = & \frac{\Theta}{Jg} + (a+ib)\omega^\alpha \Theta(\omega) \\ & + (a'+ib')|\omega|^\alpha \Theta(-\omega) + o(|\omega|^\alpha), \end{aligned} \quad (\text{B8})$$

where Θ is the Heaviside function, a, b, a', b' are real constants, and $\alpha > 0$. Then from Eq. (31b) we obtain, for $\omega > 0$,

$$\text{Im}[\tilde{\Sigma}(\omega)] = J^2 g^2 \text{Im}[2\tilde{G}(\omega) + \overline{\tilde{G}(-\omega)}] + \dots, \quad (\text{B9})$$

$$\tilde{\Sigma}(\omega) = c + [d + i(2b - b')J^2 g^2]\omega^\alpha, \quad (\text{B10})$$

where c and d are real constants. The other terms are subdominant in the limit $\omega \rightarrow 0$ as can be seen using a spectral representation. We then expand Eq. (31a) to second order and obtain at first order $\lambda = c + Jg/\Theta$ and, for the imaginary part at second order,

$$b - (2b - b')\Theta^2 = b' - (2b' - b)\Theta^2 = 0, \quad (\text{B11})$$

which leads to ($\Theta = 1$ is excluded since $b > 0$ and $b' < 0$)

$$\Theta^2 = \frac{1}{3}. \quad (\text{B12})$$

Thus the value of Θ given by the replica condition is the *only one* that leads to a gapless bosonic spectral density.

APPENDIX C: FREE ENERGY OF QUANTUM ROTOR AND ISING SPIN GLASSES

Quantum spin glasses of quantum rotors and Ising spins were studied extensively in Ref. 13. However, while the paramagnetic phase and the vicinity of the quantum-critical point were fairly completely described, the $T \rightarrow 0$ thermodynamics within the spin-glass phases was only studied in the replica-symmetric solution. A proper understanding of this low- T limit requires consideration of replica symmetry breaking, and we will provide that here. We will find, as in the more complex Heisenberg spin model considered in the body of the paper, that the specific heat is linear in T at low T .

As we are restricting our attention to mean-field theory, we can neglect the spatial dependence of all degrees of freedom. Further, we will also restrict ourselves to the Ising case, and the generalization to the multicomponent rotor case is immediate. As discussed in Ref. 13, the effective action of the quantum Ising spin glass is expressed in terms of the order parameter functional

$$Q^{ab}(\tau, \tau') = \langle \sigma^a(\tau) \sigma^b(\tau') \rangle. \quad (\text{C1})$$

where σ^a is the Ising spin in replica a . The important low-order terms in the free energy density are

$$\begin{aligned} \mathcal{F} = & \frac{1}{\kappa} \int d\tau \sum_a \left[\frac{\partial}{\partial \tau_1} \frac{\partial}{\partial \tau_2} + r \right] Q^{aa}(\tau_1, \tau_2) \Big|_{\tau_1 = \tau_2 = \tau} \\ & - \frac{\kappa}{3} \int d\tau_1 d\tau_2 d\tau_3 \sum_{abc} Q^{ab}(\tau_1, \tau_2) Q^{bc}(\tau_2, \tau_3) \\ & \times Q^{ca}(\tau_3, \tau_1) + \frac{u}{2} \int d\tau \sum_a Q^{aa}(\tau, \tau) Q^{aa}(\tau, \tau) \\ & - \frac{y}{6} \int d\tau_1 d\tau_2 \sum_{ab} [Q^{ab}(\tau_1, \tau_2)]^4. \end{aligned} \quad (\text{C2})$$

Here r is the parameter which tunes across the spin-glass transition, and κ, y measure the strength of various nonlinearities. The analysis of thermodynamic properties in the spin-glass phase in Ref. 13 was carried out with a vanishing coefficient of the quartic term, $y=0$: in this case, the order parameter has replica symmetry, and it was found that the specific heat $\sim T^3$ as $T \rightarrow 0$. Here we will extend the solution to small $y \neq 0$ and show that the solution with broken replica symmetry has a linear specific heat.

Time-translational symmetry requires that the mean-field solution take the form

$$Q^{ab}(\tau_1, \tau_2) = \frac{1}{\beta} \sum_{\nu_n} Q^{ab}(i\nu_n) e^{i\nu_n(\tau_1 - \tau_2)}. \quad (\text{C3})$$

As in Eq. (25), we choose the following ansatz for Q^{ab} :

$$Q^{ab}(i\nu_n) = \begin{cases} D(i\nu_n) + \beta q_{\text{EA}}, & a = b, \\ \beta q_{ab}, & a \neq b, \end{cases} \quad (\text{C4})$$

where the off-diagonal terms q_{ab} are time independent and characterized by the Parisi function $q(u)$, and $q(1) \equiv q_{\text{EA}}$. We have included an additive factor of βq_{EA} in the diagonal term for convenience and without loss of generality: as in the discussion below Eq. (25), we will find that this ensures that at $T=0$ the solution for $D(\tau)$ vanishes as $\tau \rightarrow \infty$. Also, the diagonal components q_{aa} do not appear in the above, and we are therefore free to choose them as $q^{aa}=0$. Here and in the remainder of this appendix, we are assuming that r is sufficiently negative so that the system has a spin-glass ground state; for larger r , the ground state is a paramagnet¹³ with $q_{\text{EA}} = q_{ab} = 0$ whose properties are not addressed here.

We now need to insert Eq. (C4) into Eq. (C2) and find the saddle point with respect to variations in the functions $q(u)$ and $D(i\nu_n)$. This is, in principle, a straightforward exercise, but the computations are somewhat lengthy.

We first identify just the terms that depend upon q^{ab} ; these have the form

$$\mathcal{F} = -R_1 \text{Tr} q^2 - \frac{R_2}{3} \text{Tr} q^3 - \frac{R_3}{6} \sum_{ab} q_{ab}^4 + \dots, \quad (\text{C5})$$

where

$$R_1 = \beta \kappa [D(0) + \beta q_{\text{EA}}],$$

$$R_2 = \kappa \beta^2,$$

$$R_3 = \beta y. \quad (\text{C6})$$

We first address the problem of determining the saddle point of Eq. (C5) with respect to variations in $q(u)$. Fortunately, this problem has been completely solved in the classical spin glass literature,³⁷ and we can directly borrow the results: the function $q(u)$ increases linearly as a function of u for $0 < u < 1 - (1 - 4R_1R_3/R_2^2)^{1/2}$, where it saturates until $u = 1$ at the constant value

$$q_{\text{EA}} = \frac{R_2 - (R_2^2 - 4R_1R_3)^{1/2}}{2R_3}. \quad (\text{C7})$$

Combining Eq. (C7) with Eq. (C5), we obtain the simple result

$$q_{\text{EA}}^2 = -\kappa D(0)/y. \quad (\text{C8})$$

Next, we consider the variation of \mathcal{F} in Eq. (C2) with respect to $D(i\nu_n)$. This is most easily done for $\nu_n \neq 0$, for which we obtain the following saddle-point equation:

$$\begin{aligned} & \frac{1}{\kappa}(\nu_n^2 + r) - \kappa D^2(i\nu_n) \\ & + u \left[\frac{1}{\beta} \sum_{\nu'_n} D(i\nu'_n) + q_{\text{EA}} \right] - 2y q_{\text{EA}}^2 D(-i\nu_n) \\ & - \frac{2y q_{\text{EA}}}{\beta} \sum_{\nu'_n} D(i\nu'_n) D(-i\nu_n - i\nu'_n) \\ & - \frac{2y}{3\beta^2} \sum_{\nu'_n, \nu''_n} d(i\nu'_n) D(i\nu''_n) D(-i\nu_n - i\nu'_n - i\nu''_n) = 0. \end{aligned} \quad (\text{C9})$$

Upon consideration of the saddle-point equation for $D(0)$, one initially finds a number of additional term associated with the coupling of $D(0)$ to q_{ab} . However, our parametrization in Eq. (C4) was chosen judiciously and has the feature that all these additional terms vanish upon using Eq. (C8); so the result (C9) applies *also* for $\nu_n = 0$.

Let us also note the complete expression for the free energy density, obtained by inserting Eqs. (C4) and (C9) into Eq. (C2):

$$\begin{aligned} \mathcal{F}/n &= \frac{q_{\text{EA}} r}{\kappa} + \frac{y^2 q_{\text{EA}}^5}{5\kappa} + \frac{1}{\beta\kappa} \sum_{\nu_n} (\nu_n^2 + r) D(i\nu_n) \\ & - \frac{\kappa}{3\beta} \sum_{\nu_n} D^3(i\nu_n) + \frac{u}{2} \left[\frac{1}{\beta} \sum_{\nu_n} D(i\nu_n) + q_{\text{EA}} \right]^2 \\ & - \frac{y q_{\text{EA}}^2}{\beta} \sum_{\nu_n} D(i\nu_n) D(-i\nu_n) \\ & - \frac{2y q_{\text{EA}}}{3\beta^2} \sum_{\nu_n, \nu'_n} D(i\nu_n) D(i\nu'_n) D(-i\nu_n - i\nu'_n) \end{aligned}$$

$$\begin{aligned} & - \frac{y}{6\beta^3} \sum_{\nu_n, \nu'_n, \nu''_n} D(i\nu_n) D(i\nu'_n) D(i\nu''_n) \\ & \times D(-i\nu_n - i\nu'_n - i\nu''_n). \end{aligned} \quad (\text{C10})$$

We are now left with the task of solving the saddle-point equations (C8) and (C9) for q_{EA} and $D(i\nu_n)$, and inserting the result into Eq. (C10). This is clearly a daunting task, and we will be satisfied in describing the $T \rightarrow 0$ limit to first order in y . This is similar in spirit to the large- S expansion of Secs. IV C 2 and IV D, and we expect that higher-order corrections in y will not modify the nature of the low- T limit.

First, we consider the case $y = 0$. Here a complete analytical solution is possible and was presented in Ref. 13. We have, at $y = 0$,

$$\begin{aligned} q_{\text{EA}}^0 &= \frac{1}{\beta\kappa} \sum_{\nu_n} |\nu_n| - \frac{r}{\kappa u}, \\ D^0(i\nu_n) &= -\frac{|\nu_n|}{\kappa}, \\ \mathcal{F}^0(T)/n &= \frac{2}{3\beta\kappa^2} \sum_{\nu_n} |\nu_n|^3 - \frac{r^2}{2\kappa^2 u} \\ &= \mathcal{F}^0(0)/n - \frac{4\pi^3 T^4}{45\kappa^2}. \end{aligned} \quad (\text{C11})$$

We observe that the free energy density behaves as T^4 , while the specific heat $\sim T^3$ as $T \rightarrow 0$. Notice also that positivity of q_{EA}^0 requires an upper bound on r , which we have assumed to hold.

Before considering explicit corrections in powers of y , we make an observation that is valid to all orders in y . The solution for $D(i\nu_n)$ in Eq. (C11), when analytically continued to real frequencies ω , has an imaginary part which vanishes linearly in ω at small ω . We now show that this conclusion holds to all orders in y ; the constraint (C8) will play a key role in establishing this result. Let us write $D(\omega) = D(0) + iD_1\omega + \dots$ for small ω , where $D(0)$ and D_1 are some real constants. Inserting this into Eq. (C9) and evaluating it at $T = 0$ for small ω , we note that the last two terms in Eq. (C9) have imaginary parts which vanish as ω^3 and ω^5 . Keeping only the leading ω dependence of the imaginary part, we obtain the simple expression

$$-2i\kappa D(0)D_1\omega - 2y q_{\text{EA}}^2 iD_1\omega = 0. \quad (\text{C12})$$

From Eq. (C8) we see that this condition is satisfied, and so D_1 can be nonzero.

Now we consider explicit first-order corrections in y : we will see that this leads to terms in the thermodynamics which vanish more slowly as $T \rightarrow 0$. We can easily use Eqs. (C8) and (C9) to determine the corrections to $D(i\nu_n)$ and q_{EA} to linear order in y ; however, these are not needed here as the shift in the free energy due to such corrections will only appear at order y^2 , because the free energy is at a saddle point. Indeed, to obtain the free energy correct to first order in y , we need only insert Eq. (C11) into Eq. (C10). It is then

quite easy to see that the free energy will have a term of order yT^2 and that the coefficient of this term will be non-universal and dependent upon the nature of the high-energy cutoff. The required term comes from the T dependence of q_{EA}^0 , which from Eq. (C11) is seen to be

$$q_{\text{EA}}^0(T) = q_{\text{EA}}^0(0) - \frac{\pi T^2}{3\kappa}. \quad (\text{C13})$$

Upon inserting Eqs. (C13) and (C11) into Eq. (C10), we will now obtain numerous terms in which the above T^2 term multiplies T -independent, cutoff-dependent terms coming from the upper bounds in the summations over the $D(i\nu_n)$. As the relative values of these contributions will depend upon the nature of the cutoff, there is no general reason for them to cancel against each other. Hence we obtain a T^2 contribution to \mathcal{F} and a linear T term in the low- T specific heat.

-
- ¹Proceedings of the Conference on Non-Fermi Liquid Behavior in Metals [J. Phys.: Condens. Matter **8**, 9675 (1996)].
- ²P. Coleman, Physica B **259–261**, 353 (1999).
- ³S. Doniach, Physica B **91**, 213 (1977).
- ⁴J. Hertz, Phys. Rev. B **14**, 1165 (1976).
- ⁵A. Millis, Phys. Rev. B **48**, 7183 (1993).
- ⁶S. Sachdev, N. Read, and R. Oppermann, Phys. Rev. B **52**, 10 286 (1995).
- ⁷A. Sengupta and A. Georges, Phys. Rev. B **52**, 10 295 (1995).
- ⁸S. Sachdev, *Quantum Phase Transition* (Cambridge University Press, Cambridge, England, 1999).
- ⁹S. Sachdev, A. Chubukov, and A. Sokol, Phys. Rev. B **51**, 14 874 (1995).
- ¹⁰S. Sachdev and A. Georges, Phys. Rev. B **52**, 9520 (1995).
- ¹¹A. Sengupta, Phys. Rev. B **61**, 4041 (2000).
- ¹²J. Smith and Q. Si, Phys. Rev. B **61**, 5184 (2000).
- ¹³N. Read, S. Sachdev, and J. Ye, Phys. Rev. B **52**, 6411 (1995).
- ¹⁴R. Bhatt, in *Spin Glasses and Random Fields*, edited by A. P. Young (World Scientific, Singapore, 1997).
- ¹⁵J. Miller and D. A. Huse, Phys. Rev. Lett. **70**, 3147 (1993).
- ¹⁶D. Fisher, Phys. Rev. B **51**, 6411 (1995).
- ¹⁷C. Pich *et al.*, Phys. Rev. Lett. **81**, 5916 (1998).
- ¹⁸O. Motrunich, S. Mau, D. Huse, and D. Fisher, Phys. Rev. B **61**, 1160 (2000).
- ¹⁹S. Sachdev and J. Ye, Phys. Rev. Lett. **70**, 3339 (1993).
- ²⁰A. Georges, O. Parcollet, and S. Sachdev, Phys. Rev. Lett. **85**, 840 (2000).
- ²¹A. Bray and M. Moore, J. Phys. C **13**, L655 (1980).
- ²²M. Mézard, G. Parisi, and M. Virasoro, *Spin Glass Theory and Beyond* (World Scientific, Singapore, 1987).
- ²³T. Kopeć, Phys. Rev. B **52**, 9590 (1995).
- ²⁴D. Grepel and M. Rozenberg, Phys. Rev. Lett. **80**, 389 (1998).
- ²⁵O. Parcollet and A. Georges, Phys. Rev. B **59**, 5341 (1999). In this paper only the fermionic model is considered, but the results apply also to the paramagnet in the bosonic model (with minor changes).
- ²⁶O. Parcollet, A. Georges, G. Kotliar, and A. Sengupta, Phys. Rev. B **58**, 3794 (1998).
- ²⁷O. Parcollet and A. Georges, Phys. Rev. Lett. **79**, 4665 (1997).
- ²⁸S. Sachdev, C. Buragohain, and M. Vojta, Science **286**, 2479 (1999).
- ²⁹M. Vojta, C. Buragohain, and S. Sachdev, Phys. Rev. B **61**, 15 152 (2000).
- ³⁰D. Forster, D. Nelson, and M. Stephen, Phys. Rev. A **16**, 732 (1977).
- ³¹J. Honkonen and E. Karjalainen, J. Phys. A **21**, 4217 (1988). For a review see also J. P. Bouchaud and A. Georges, Phys. Rep. **195**, 127 (1990).
- ³²M. Mézard and G. Parisi, J. Phys. I **1**, 809 (1991).
- ³³T. Giamarchi and P. Le Doussal, Phys. Rev. B **53**, 15 206 (1996).
- ³⁴L. Cugliandolo, C. Da Silva Santos, and D. Grepel, cond-mat/0003268 (unpublished).
- ³⁵L. Cugliandolo and G. Lozano, Phys. Rev. B **59**, 915 (1999).
- ³⁶A. de Almeida and D. Thouless, J. Phys. A **11**, 983 (1978), reprinted in Ref. 22.
- ³⁷K. Fischer and J. Hertz, *Spin Glasses* (Cambridge University Press, Cambridge, England, 1993).